JOHNSON MATTHEY
TECHNOLOGY REVIEW
www.technology.matthey.com

# Johnson Matthey Highlights

**A selection of recent publications by Johnson Matthey R&D staff and collaborators**

## A Novel Integrated Biorefinery Process for Diesel Fuel Blendstock Production Using Lipids from the Methanotroph, *Methylomicrobium buryatense*

T. Dong, Q. Fei, M. Genelot, H. Smith, L. M. L. Laurens, M. J. Watson and P. T. Pienkos, *Energy Convers. Manage.*, **140**, 62

A technically feasible biological gas-to-liquid fuel (bio-GTL) process is demonstrated for the first time. The aerobic methanotrophic bacterium, *Methylomicrobium buryatense*, was used to produce a maximum fatty acid content of 10% of dry cell weight from $CH_4$ in batch cultures in a continuous gas sparging fermentation system. Novel lipid extraction methodology with advanced catalyst design was then used to prove the feasibility of upgrading phospholipids to hydrocarbon fuels. Up to 95% of the fatty acids were recovered by two-stage pretreatment and hexane extraction of the aqueous hydrolysate. The extracted lipids were then upgraded by hydrodeoxygenation using a palladium on silica catalyst. The final hydrocarbon mixture is 88% pentadecane.

## Heavy Duty Diesel Engine Emission Control to Meet BS VI Regulations

S. Chatterjee, M. Naseri and J. Li, SAE Technical Paper 2017-26-0125, 2017

From 2020 the BS VI emission regulations in India will require both advanced NOx control and advanced PM control along with particle number limitations. This will require implementation of full diesel particulate filter (DPF) and simultaneous NOx control using SCR technologies. This presentation gives an overview of various DOC, DPF and SCR catalyst technologies and their applications, with respect to their implementation for BS VI HDD regulations. DPF technologies have already been implemented in systems for the Euro VI and US 10 HDD regulations.

## Quantitative 3D Visualization of the Growth of Individual Gypsum Microcrystals: Effect of $Ca^{2+}$:$SO_4^{2-}$ Ratio on Kinetics and Crystal Morphology

M. M. Mbogoro, M. Peruffo, M. Adobes-Vidal, E. L. Field, M. A. O'Connell and P. R. Unwin, *J. Phys. Chem. C*, 2017, **121**, (23), 12726

The present study elucidates the influence of the ratio of $Ca^{2+}$ to $SO_4^{2-}$ ions at constant supersaturation on the rate of growth at the major crystal faces of gypsum. The 3D time-evolution of microcrystals are measured by *in situ* AFM and these measurements are coupled to a diffusion model. The growth rate at the {100} and {001} faces is found to be highly sensitive to solution stoichiometry, with needle-like crystals forming in $Ca^{2+}$-rich solutions and plate-like crystals forming in $SO_4^{2-}$-rich solutions. The highest growth rate was found using a stoichiometric solution of $Ca^{2+}$:$SO_4^{2-}$.

## Unravelling the Mystery of Palladium Acetate

W. Carole and T. Colacot, *Chim. Oggi*, 2017, **35**, (3), 64

$Pd_3(OAc)_6$, **1**, is used to catalyse organic transformations such as C–H activation and cross-coupling and is used for manufacturing pharmaceuticals and agrochemicals. There are two typical impurities found in commercial samples. This study systematically investigates high purity palladium acetate, **1**, and the two main impurities: palladium acetate nitrite, **2**, and polymeric palladium acetate, **3**. **3** was found to be just as active as **1** or **2** under specific conditions, but shows reduced performance at lower temperatures and in the absence of a phosphine ligand. In pre-catalyst manufacture, pure **1** gave the best yield and purity, and hence may be the ideal choice for reliable results.

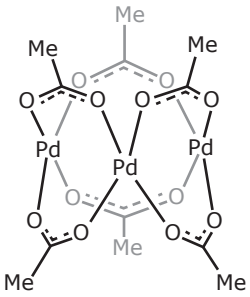

$Pd_3(OAc)_6$

**1**

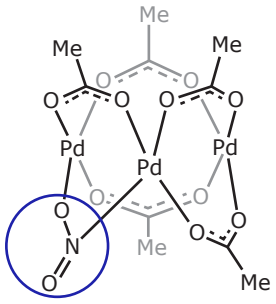

$Pd_3(OAc)_5(NO_2)$

**2**

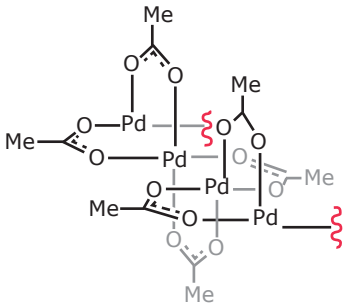

$(Pd(OAc)_2)_n$

**3**

W. Carole and T. Colacot, *Chim. Oggi*, 2017, **35**, (3), 64

## Full Deflection Profile Calculation and Young's Modulus Optimisation for Engineered High Performance Materials

A. Farsi, A. D. Pullen, J. P. Latham, J. Bowen, M. Carlsson, E. H. Stitt and M. Marigo, *Sci. Rep.*, 2017, **7**, 46190

The effects of microstructural design and sintering process used in the manufacture of engineered materials for additive manufacturing applications in medicine, engineering and technology are studied. A new methodology is presented which shows that the full deflection profile can be calculated from video recordings of bending tests, Young's modulus can be characterised by an optimisation algorithm and optical distortions can be quantified. The results are compared with other standard tests. The new procedure allows the Young's modulus of highly stiff materials to be evaluated with greater accuracy than possible with previous bending tests and extends to this class of materials the possibility to evaluate both the elastic modulus and the tensile strength with a single mechanical test.

## Enhanced MEA Performance for PEMFCs under Low Relative Humidity and Low Oxygen Content Conditions *via* Catalyst Functionalization

L. Xin, F. Yang, J. Xie, Z. Yang, N. N. Kariuki, D. J. Myers, J.-K. Peng, X. Wang, R. K. Ahluwalia, K. Yu, P. J. Ferreira, A. M. Bonastre, D. Fongalland and J. Sharman, *J. Electrochem. Soc.*, 2017, **164**, (6), F674

A new way to enhance catalyst performance for the next generation of catalytic materials for PEMFCs is demonstrated. Functionalised annealed-Pt/Ketjen black EC300j (a-Pt/KB) and dealloyed-PtNi/Ketjen black EC300j (d-PtNi/KB) catalysts using p-phenyl sulfonic acid improved the performance of MEAs in PEMFCs. The size of Pt and PtNi catalyst particles was increased and there was additional leaching of Ni from the PtNi catalyst. Formation of nanoporous PtNi nanoparticles was promoted. Catalyst layers with narrower pore size distributions were formed. Improved high current density performance was observed under reduced RH conditions especially when using reactant gases with low relative humidity.

## Reverse Monte Carlo Studies of $CeO_2$ using Neutron and Synchrotron Radiation Techniques

A. H. Clark, H. R. Marchbank, T. I. Hyde, H. Y. Playford, M. G. Tucker and G. Sankar, *Phys. Scr.*, 2017, **92**, (3), 034002

The structure of a crystalline $CeO_2$ was extracted by a reverse Monte Carlo analysis from neutron total scattering (consisting of both neutron diffraction and pair-distribution functions) and $CeL_3$- and K-edge EXAFS data. A notable difference was observed between using short ranged X-ray absorption spectroscopy data and using medium long range pair-distribution functions and neutron diffraction data regarding the disorder of Ce atoms. This demonstrates the significance of studying multiple length scales and radiation sources.

## Understanding and Overcoming the Limitations of *Bacillus badius* and *Caldalkalibacillus thermarum* Amine Dehydrogenases for Biocatalytic Reductive Amination

A. Pushpanath, E. Siirola, A. Bornadel, D. Woodlock and U. Schell, *ACS Catal.*, 2017, **7**, (5), 3204

The kinetic and thermostability parameters were investigated for a newly engineered amine dehydrogenase from a phenylalanine dehydrogenase from *Caldalkalibacillus thermarum* and were compared against an existing amine dehydrogenase from *Bacillus badius*. The former showed an increased thermostability (melting temperature, $T_m$) of 83.5ºC compared to 56.5ºC for the latter. This newly engineered enzyme was also

used in the reductive amination of up to 400 mM of phenoxy-2-propanone ($c$ = 96%, ee ($R$) <99%) in a biphasic reaction system using a lyophilised whole-cell preparation. The lower turnover number of the existing amine dehydrogenase compared to their phenylalanine dehydrogenase counterpart was studied by computational docking simulations.

### Key Considerations for High Current Fuel Cell Catalyst Testing in an Electrochemical Half-Cell

B. A. Pinaud, A. Bonakdarpour, L. Daniel, J. Sharman and D. P. Wilkinson, *J. Electrochem. Soc.*, 2017, **164**, (4), F321

An economical and novel half-cell method for swiftly and accurately measuring oxygen reduction catalysts in different practical electrode formats, including GDE and bonded GDE/membrane layers is shown. The challenges in developing such a test platform were highlighted with a concise summary of key design considerations and fuel cell current densities of ~1 A $cm^{-2}$ were achieved. A simple, reproducible process of measuring catalyst performance was provided by constant current polarisations with IR drop measurement at each stage. At a substantially lower testing cost the ORR activity of commercial products was accurately provided by the half-cell used in this study and showed good agreement with measurements made in fuel cell hardware. Many types of GDE and CCM with different catalyst layers can be characterised by this half-cell method.

### Mild $sp^2$Carbon–Oxygen Bond Activation by an Isolable Ruthenium(II) Bis(dinitrogen) Complex: Experiment and Theory

S. Lau, B. Ward, X. Zhou, A. J. P. White, I. J. Casely, A. A. Macgregor and M. R. Crimmin, *Organometallics*, 2017, **36**, (18), 3654

At temperatures below 40ºC the isolable ruthenium(II) bis(dinitrogen) complex $[Ru(H)_2(N_2)_2(PCy_3)_2]$ reacts with aryl ethers (Ar–OR, R = Me and Ar) comprising a ketone directing group to achieve $sp^2$C–O bond activation. The oxidative addition of the C–O bond to Ru(II) happens in an asynchronous manner with Ru–C bond formation prior to C–O bond breaking in a low energy Ru(II)/Ru(IV) pathway for C–O bond activation, was concluded by DFT studies. $sp^2$C–H bond activation was demonstrated to be more simplistic compared to $sp^2$C–O bond activation by experiments and DFT calculations.

### Combined *In Situ* XAFS/DRIFTS Studies of the Evolution of Nanoparticle Structures from Molecular Precursors

E. K. Dann, E. K. Gibson, R. A. Catlow, P. Collier, T. E. Erden, D. Gianolio, C. Hardacre, A. Kroner, A. Raj, A. Goguet and P. P. Wells, *Chem. Mater.*, 2017, **29**, (17), 7515

The formation of PdO nanoparticles from two different impregnated Pd precursors, $Pd(NO_3)_2$ and $Pd(NH_3)_4(OH)_2$ were studied, and was captured by a spectroscopic method for advanced *in situ* characterisation. The temperature assisted pathway for ligand decomposition was identified by time-resolved diffuse reflectance infrared Fourier transform spectroscopy which demonstrated that $NH_3$ ligands are oxidised to $N_2O$ and $NO^-$ species but $NO_3^-$ ligands help join Pd centres *via* bidentate bridging coordination. By using this spectroscopic method in conjunction with simultaneous X-ray absorption fine structure spectroscopy, the following nucleation and growth mechanisms of the previous metal oxide nanoparticles were determined. The formation and growth of larger PdO nanoparticles at lower onset temperature (<250ºC) was assisted by the bridging capability of $Pd(NO_3)_2$. However, impregnation from $[Pd(NH_3)_4]^{2+}$ results in well isolated Pd centres attached to the support which needs a higher temperature (>360ºC) for migration to develop observable Pd–Pd distances of PdO nanoparticles.

### Electrochemical and Spectroscopic Characterization of an Alumina-coated $LiMn_2O_4$ Cathode with Enhanced Interfacial Stability

M. Pasqualini, S. Calcaterra, F. Maroni, S. J. Rezvani, A. Di Cicco, S. Alexander, H. Rajantie, R. Tossici and F. Nobili, *Electrochim. Acta*, 2017, **258**, 175

The electrochemical performances and stability of the $LiMn_2O_4$ cathode at high temperatures were enhanced by pristine $LiMn_2O_4$ which was synthesised by solid state route and coated by an $Al_2O_3$ layer through co-precipitation process. A pure phase and crystallised nanomaterial forming clusters were observed by XRD, scanning and transmission electron microscopy. Galvanostatic cycles at several charge/discharge rates were used to study the cycling performances of pristine and modified materials. A combination of galvanostatic cycles at 1C and electrochemical impedance spectroscopy at T = 25ºC and T = 50ºC show that the electrode/electrolyte interface of $Al_2O_3$-modified $LiMn_2O_4$ is stabilised by suppressing Mn dissolution which exhibits improved cycleability particularly at high temperatures.